Transition metal catalyzed oxidation of Alcell lignin, soda lignin, and lignin model compounds in ionic liquids

Joseph Zakzeski, Anna L. Jongerius and Bert M. Weckhuysen*

Received 21st January 2010, Accepted 23rd March 2010
First published as an Advance Article on the web 24th May 2010
DOI: 10.1039/c001389g

Lignin is a component of lignocellulosic biomass from which important aromatic compounds can potentially be obtained. In the present work, Alcell and soda lignin were dissolved in the ionic liquid 1-ethyl-3-methylimidazolium diethylphosphate (EMIM DEP) and subsequently oxidized using several transition metal catalysts and molecular oxygen under mild conditions. $CoCl_2 \cdot 6H_2O$ in EMIM DEP proved particularly effective for the oxidation. The catalyst rapidly oxidized benzyl and other alcohol functionalities in lignin, but left phenolic functionality and 5–5′, β-*O*-4 and phenylcoumaran linkages intact, as determined by analysis of various lignin model compounds and ATR-IR spectroscopy. The catalyst system oxidized the alcohol functionality contained in cinnamyl alcohol to form cinnamaldehyde or cinnamic acid or disrupted the double bond to form benzoic acid or an epoxide. The benzyl functionality in veratryl alcohol, a simple non-phenolic lignin model compound, was selectively oxidized to form veratraldehyde at a maximum turnover frequency of 1440 h^{-1}, compared to 10–15 h^{-1} reported for earlier systems. Phenolic functional groups contained in guaiacol, syringol, and vanillyl alcohol remained intact, although the benzyl alcohol group in the latter was oxidized to form vanillin. Incorporation of strongly bound tetradentate ligands to the catalyst yielded reduced activity relative to those derived from simple metal salts in EMIM DEP. The influence of reaction conditions, such as temperature, oxygen pressure and NaOH loading, were also investigated. The system represents a potential method in a biorefinery scheme to increase the oxygen functionality in lignin prior to depolymerization or additional functionalization of already depolymerized lignin.

1. Introduction

Lignocellulosic biomass is a renewable resource that has the potential to serve as a feedstock for the production of fuels, chemicals, and energy.[1] This biomass consists of three major components – cellulose, hemicelluloses, and lignin – each with unique physical, chemical, and structural properties that offer specific opportunities to produce a multitude of valuable chemicals.[2] In particular, lignin is a three-dimensional amorphous polymer consisting of methoxylated phenylpropane structures from which high-value aromatic molecules can potentially be obtained.[3] In plants, it constitutes up to 30% by weight and 40% by energy of lignocellulosic biomass.[4] It fills the spaces between the cellulose and hemicellulose, and it acts as a resin to confer strength and rigidity to the plant.[5] This same rigidity and strength, however, complicates the valorization of lignin and the other components of lignocellulosic biomass by making it resistant to chemical transformation. With the depletion of fossil fuels as a source of fuels, chemicals, and energy, the need to develop processes to efficiently valorize lignin and the other components of biomass to renewable energy and chemicals is becoming increasingly important.

Utrecht University, Sorbonnelaan 16, Utrecht, The Netherlands. E-mail: b.m.weckhuysen@uu.nl

Dissolution of wood and other lignocellulosic material is a critical step for the valorization of biomass.[1] In fact, the insolubility of wood in common solvents has severely inhibited the development of processes for wood and lignocellulosic biomass valorization.[1] Although several strategies involving solvents such as DMSO[6] or CO_2-expanded organic solvents[7] have been employed to dissolve lignocellulosic material, ionic liquids in particular have recently become popular solvents for the dissolution of biomass, and several types are commercially available.[8] Some of the most common types are EMIM (1-ethyl-3-methylimidazolium) or BMIM (1-butyl-3-methylimidazolium) with various anionic counterions.[8] The physical properties of these ionic liquids are highly dependent on the cation–anion pair. Because of their good thermal stability and negligible vapor pressure, ionic liquids are regarded as "green solvents" that could potentially replace volatile organic solvents.[9,10] Importantly, several recent studies have demonstrated the effectiveness of ionic liquids for the dissolution of wood and lignocellulosic biomass.[10–15] Vitz and coworkers, for example, noted that 1-ethyl-3-methylimidazolium diethyl phosphate (EMIM DEP) in particular was an excellent solvent for the dissolution of cellulose.[16] Zakrzewska and coworkers recently published a review of the solubility of carbohydrates, including lignin, in ionic liquids, noting that the highest solubility of lignin is obtained in 1,3-dimethylimidazolium methanesulfonate (MMIM CH_3SO_3).[17]

Once dissolved in the ionic liquid, lignocellulosic material is susceptible to a wide range of transformations including acetylation,[18] acid hydrolysis,[19,20] acylation,[21] reduction,[22] and enzymatic oxidations using horseradish peroxidase.[23] Although there are several examples of catalysts capable of using molecular oxygen for the oxidation of lignin (or lignin-related model compounds), such as heterogeneous[24–26] and homogeneous[27–32] transition metal catalysts (Co(porphyrin),[33] Co(salen)[34–39] and polyoxometalate[40–49]), to the best of our knowledge there are currently no examples of catalytic oxidative lignin valorization using molecular oxygen with ionic liquids as the solvent.[1] Since molecular oxygen is a cheap and abundant oxidant, the development of such a process would be attractive for future utilization in lignin valorization processes. In addition, there are several properties of ionic liquids that could make them an attractive medium for lignin oxidative valorization. They have high gas solubility[50,51] and the ability to dissolve lignocellulosic materials including wood and the products derived therefrom. There is often a beneficial effect of pyridine and imidazole on catalytic performance, particularly for Co(salen) and Co porphyrin catalysts,[52,53] and imidazole impurities are often in high abundance in imidazolium-based ionic liquids. Moreover, ionic liquids are an environmentally-friendly solvent choice for the production of renewable chemicals. The challenge, therefore, is to identify an ionic liquid and catalyst pair capable of selectively valorizing lignin, or components derived from its depolymerization, using molecular oxygen as the oxidant.

Motivated by these impetuses, the objective of this work was to investigate the performance of Co(salen), Co(porphyrin) and similar catalysts for lignin oxidation in ionic liquids using molecular oxygen. Inspired by the effective dissolution of cellulose by EMIM DEP,[16] we extended this ionic liquid to the dissolution of lignin and performed the catalytic oxidation of dissolved lignin in this medium. In order to better understand the chemical transformations that occur during lignin oxidation, we investigated the reactivity of the catalytic system towards several lignin model compounds that exhibit the salient linkages and functionalities contained in lignin. We also analyzed the influence of reaction conditions on catalytic performance and attempted to determine the important components in the ionic liquid–catalyst system.

2. Experimental

2.1 Typical reactions

Alcell™ Organosolv lignin was obtained from Repap Technologies Inc., Valley Forge, PA, USA. This lignin was extracted from mixed hardwoods (maple, birch, and poplar) by an organosolv process using aqueous ethanol. Soda lignin was extracted from grass and was obtained from the Energy Research Centre of The Netherlands (ECN).

Reactions were conducted in a 40 mL Parr stainless steel autoclave. The temperature was monitored using a thermocouple, and stirring was conducted using a magnetic driver equipped with an impellor at 750 rpm. Reactions were conducted as follows (unless noted otherwise): into a 10.00 g sample of 1-ethyl-3-methylimidazolium diethyl phosphate (EMIM DEP, Io-li-tec, >98%) was dissolved 10 μmol Co(salen) (0.0032 g, Aldrich, 99%) or $CoCl_2 \cdot 6H_2O$ (0.0024 g, Acros Organics), along with 2 mmol NaOH (0.080 g, Aldrich, 97%). The solution was stirred overnight in order to completely dissolve the catalyst. The designated substrate, typically 4.15 mmol veratryl alcohol (0.698 g, Aldrich, 96%), was dissolved in the reaction solution, which was then transferred to the autoclave and sealed. If the reaction involved solid substrates or lignin samples, these substrates were also dissolved in the ionic liquid by stirring overnight to obtain a homogeneous solution. In some cases, the impurities contained in the substrates consisted of the oxidized product (*i.e.* veratraldehyde in the case of veratryl alcohol), and these impurities were quantified and catalytic performance calculations were adjusted accordingly. Before conducting a reaction, the autoclave was purged four times with oxygen. The autoclave was then charged with oxygen (0.5 MPa, Hoekloos, 99.5%) and heated to 353 K over about 5 min. After a designated reaction time, the autoclave was cooled to 333 K, vented, and a 1.0 g sample was taken. The autoclave was again purged with oxygen, recharged with 0.5 MPa O_2, and re-heated to 353 K. Between reactions, the autoclave was thoroughly washed with water and ethanol, rinsed with acetone or ethanol, and dried.

Products and residual substrate were separated from the ionic liquid by five sequential extractions using 1.35 g ethyl acetate. Prior to conducting reactions, extraction efficiencies of the potential reaction components (*i.e.* veratryl alcohol, veratraldehyde, vanillin, vanillyl alcohol, *etc.*) using ethyl acetate or diethyl ether were determined. Both ethyl acetate and diethyl ether efficiently extracted the substrate and products from the ionic liquids, but extraction efficiencies were generally higher when ethyl acetate was used, compared to diethyl ether. Two distinct liquid phases formed when both of these solvents were combined with EMIM DEP, and the top ethyl acetate phase was decanted and analyzed. Higher mixing was observed with many of the other ionic liquids, such as BMIM PF_6, requiring centrifugation prior to decantation.

Product quantification was conducted using a Shimadzu GC-2010A gas chromatography unit equipped with a WCOT fused silica CP-WAX 57CB column. Products were identified using a Shimadzu GCMS-QP2010 unit or a LCMS-2010EV unit with acetonitrile and 10 mM ammonium acetate in water as solvents, and compared with pure standards when available.

2.2 Lignin model compound synthesis

The 5–5′ model compound, 3,3′-dimethoxy-5,5′-dimethyl-1,1′-biphenyl-2,2′-diol, was synthesized as reported in the literature.[54,55] The product was repeatedly purified using a silica gel column using hexanes and ethyl acetate (1 : 3) as the solvent, and then crystallized. The purity was checked using ^{1}H NMR. The β-*O*-4 compound 1-hydroxy-1-(4-hydroxy-3-methoxyphenyl)-2-(2,6-dimethoxyphenoxy)ethane was synthesized as reported in the literature for the synthesis of 1,3-dihydroxy-1-(3,5-dimethoxy-4-hydroxyphenyl)-2-(2,6-dimethoxyphenoxy)propane, except that the paraformaldehyde was not added to the 1-(4-benzoyloxy-2,5-dimethoxyphenyl)-2-(2,6-dimethoxyphenoxy)ethanone during the synthesis.[56] The compound was similarly purified using a silica gel column with hexanes and ethyl acetate (1 : 3) as the solvent, repeatedly crystallized, and the purity checked using ^{1}H NMR.

2.3 Spectroscopy

UV-visible spectroscopy was conducted using a Varian Cary 50 Conc UV-visible spectrometer equipped with an immersion probe. During a measurement, 0.1 g of sample was placed in a vial and diluted with 1.9 g ethanol. The immersion probe with a 1 mm path length was placed in the solution, and the UV-visible spectrum was recorded with pure ethanol as the background. Infrared spectroscopy was conducted at room temperature using a Perkin Elmer System 2000 FT-IR equipped with a Pike Technologies MIRacle™ single-reflection horizontal ATR accessory.

3. Results and discussion

3.1 Lignin oxidation

The oxidation of two types of lignin, Alcell lignin and soda lignin, was investigated using a $CoCl_2 \cdot 6H_2O$ catalyst dissolved in EMIM DEP. As depicted in Fig. 1, which is a schematic representation of hardwood lignin, the lignin polymer contains several alcohol functional groups that are susceptible to oxidations and also several types of linkages that, if successfully cleaved would potentially result in low molecular weight aromatic products. Both the Alcell lignin and soda lignin readily dissolved in EMIM DEP to yield dark brown solutions. Samples were taken each hour, and a small portion of each sample was saved for spectroscopic analysis. Analysis of the reaction solution was conducted by first performing ethyl acetate extractions in an attempt to isolate any possible low molecular weight, monomeric products formed during the reaction; however, no monomeric products were detected by GC-MS. The lignin reaction samples were then analyzed by ATR-IR in an attempt to observe evidence of lignin oxidation. The results are depicted in Fig. 2, which displays the difference in the ATR-IR spectra between the lignin solution after various reaction times and the lignin solution prior to reaction. Two new peaks appeared near 3255 cm^{-1} and 1654 cm^{-1} that increased in intensity with increasing reaction time. These peaks correspond to the region of the infrared spectrum associated with alcohol and aldehyde stretches, respectively, which suggests that the dissolved lignin was selectively oxidized by the catalyst. The absence of monomeric products, however, suggests either that the linkages in the lignin remained intact or were insufficiently disrupted to yield aromatic products of sufficiently low molecular weight for GC-MS detection.

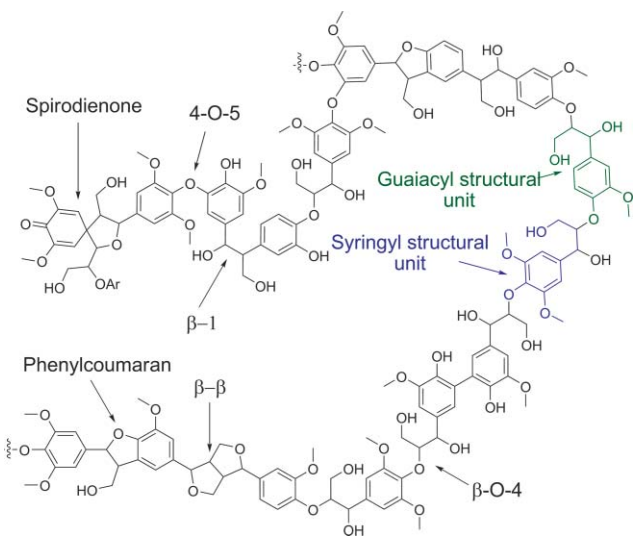

Fig. 1 Schematic representation of hardwood lignin.[1]

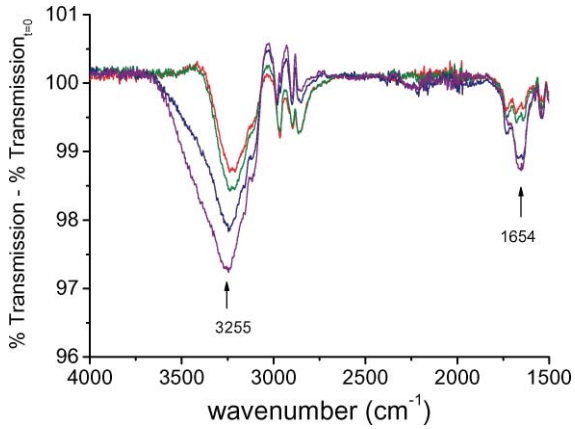

Fig. 2 Difference in ATR-IR spectra between the soda lignin after various reaction times and the lignin solution prior to reaction: (—) t = 1 h; (—) t = 2 h; (—) t = 3 h; (—) t = 4 h.

3.2 Lignin model compounds mimicking the linkages of lignin

In order to gain increased insight into the transformations occurring within the lignin samples by the catalyst and to bypass the analytical challenges associated with the lignin polymer, additional analysis was conducted by the reaction of several lignin model compounds that mimic the salient features of lignin. Lignin contains several linkages, the most common of which include β-*O*-4, 5–5′, and β-5, throughout its structure with the relative content depending on the plant material and pretreatment method.[1] Several model compounds were therefore synthesized and used to investigate the reactivity of these linkages to the $CoCl_2 \cdot 6H_2O$ in EMIM DEP. Schematic representations of the model compounds used to analyze the β-*O*-4, 5–5′, and β-5 linkages are depicted in Fig. 3. 2,3-Dihydrobenzofuran (compound **1**, Fig. 3) represents the simplest model compound that resembles phenylcoumaran linkages. No reaction was observed after 4 h with this compound, and the starting material was completely recovered. These results indicate that phenylcoumaran linkages are expected to remain intact during the oxidation of lignin.

Analysis of the 5–5′ carbon–carbon bond was conducted using the compound 3,3′-dimethoxy-5,5′-dimethyl-1,1′-biphenyl-2,2′-diol (compound **2**, Fig. 3). After 4 h at 353 K, neither 4-hydroxy-3-methoxytoluene nor similar monomeric products were detected, indicating that the carbon–carbon bond linking the dimers remained intact. Interestingly, two products in approximately equal proportion were detected that corresponded to approximately 50% conversion of the starting material after 4 h. GC-MS analysis of the products revealed masses of 288 and 302 daltons, which possibly corresponded to the oxidation of the methyl groups on the dimer to the corresponding aldehyde. Most likely, the reaction proceeds through the oxidation of the methyl group to form the alcohol, which is then rapidly oxidized

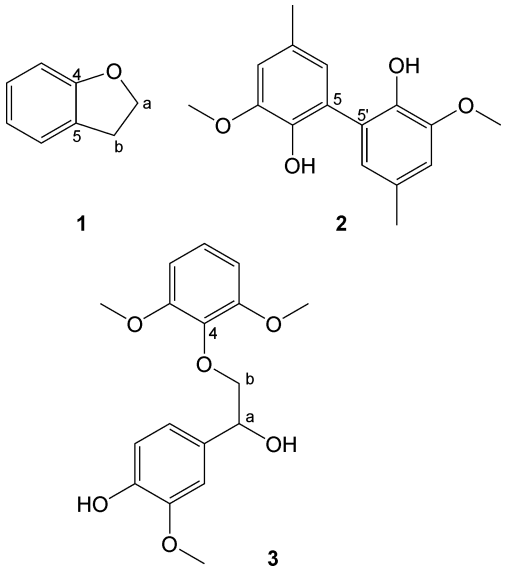

Fig. 3 Lignin model compounds used to mimic the (1) phenylcoumaran β-5, (2) 5–5′, and (3) β-*O*-4 linkages of the lignin samples.

to the aldehyde. Similarly to the other phenolic compounds, no quinones were detected as products.

The β-*O*-4 linkage is the most common found in lignin, and the lignin model compound 1-hydroxy-1-(4-hydroxy-3-methoxy-phenyl)-2-(2,6-dimethoxyphenoxy)ethane (compound **3**, Fig. 3) was used to model these linkages. As with the other linkages of lignin, no evidence of syringol, apocynol or related compounds expected from the rupture of the β-*O*-4 bond were detected by GC-MS after reaction. Analysis of the same solution by LC-MS revealed the oxidation of approximately 85% of the alcohol functionality in the compound to the corresponding ketone, as indicated in Scheme 1. No other products were detected.

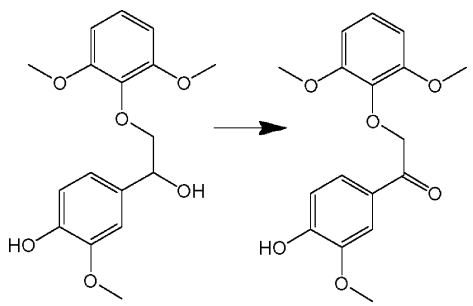

Scheme 1 Oxidation of the β-*O*-4 lignin model compound.

3.3 Lignin model compounds mimicking the functional groups of lignin

In addition to the various linkages, both phenolic and non-phenolic structures are present in lignin, as well as variations on the propyl-side chain depending on the pretreatment method in which the lignin was prepared.[1] In order to determine the effect of the catalyst system on the substituent groups in lignin, the catalyst system was applied to several lignin model compounds, schematic representations of which are depicted in Fig. 4.

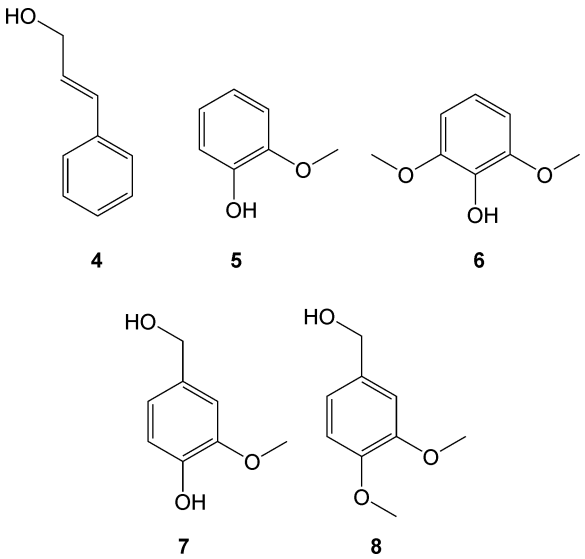

Fig. 4 Lignin model compounds used to mimic the propyl side-chain (**4**), the phenolic (**5**, **6**, **7**) and nonphenolic (**8**) functional groups of lignin.

Cinnamyl alcohol (compound **4**, Fig. 4) exhibits a propyl side-chain containing a carbon–carbon double bond, which is occasionally observed in lignin streams based on the pre-treatment method, and a C_γ–OH functionality. The reaction of this substrate was therefore conducted to gain insight into the reactivity of the catalytic system towards the propyl side chain. The results of the cinnamyl alcohol oxidation using the catalyst system are depicted in Fig. 5. Initially, cinnamyl alcohol was oxidized to cinnamaldehyde leaving the carbon–carbon double bond intact. As the reaction proceeded, several other products were observed including benzoic acid and cinnamic acid. Epoxidation of the double bond was also observed. After two hours, the yield of cinnamaldehyde began to decrease, whereas the quantity of the other products continued to increase. The quantity of benzoic acid and cinnamic acid formed corresponded to the decrease in the cinnamaldehyde yield,

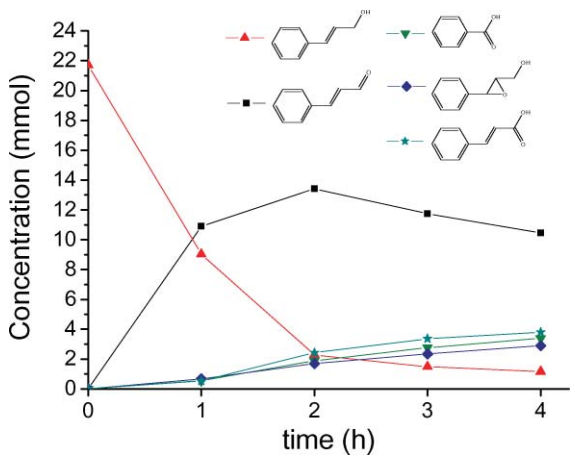

Fig. 5 $CoCl_2 \cdot 6H_2O$-catalyzed cinnamyl alcohol oxidation: mmol of substrate and products *versus* time. Reaction conditions: 5.00 g EMIM DEP, 10 μmol $CoCl_2 \cdot 6H_2O$ (0.0024 g), 1 mmol NaOH (0.04 g), 21.7 mmol cinnamyl alcohol (2.912 g), 0.5 MPa O_2 (continuous), T = 353 K.

suggesting that these products are also formed as a result of a series of reactions, whereby high substrate concentrations favor their formation. Interestingly, formation of the cinnamaldehyde was initially favored over the formation of the epoxide; however, as the quantity of substrate began to diminish, cinnamaldehyde formation decreased significantly while the epoxide formation continued unabated. These species are likely formed by a different mechanism, in which the aldehyde rate is strongly related to substrate concentration, whereas the epoxide is largely independent.

The model compounds guaiacol (3-methoxyphenol) (**5**), syringol (2,6-dimethoxyphenol) (**6**) and vanillyl alcohol (4-hydroxy-3-methoxybenzyl alcohol) (**7**) were chosen as representative phenolic lignin model compounds. Guaiacol and syringol contain common functionalities observed in softwood and hardwood lignin, respectively, without the presence of other complicating functionalities. Without the extra methoxy functionality serving as a protecting group, these compounds are susceptible to oxidation to form benzoquinones. These substrates, however, failed to react in the presence of $CoCl_2 \cdot 6H_2O$ in EMIM DEP, and the original substrate was completely recovered. As indicated in Fig. 6, the alcohol functionality of vanillyl alcohol was successfully oxidized to form vanillin. As in the case of guaiacol and syringol, the phenol component of this compound remained intact; no quinones were detected. No vanillic acid was detected; vanillin was the only product observed.

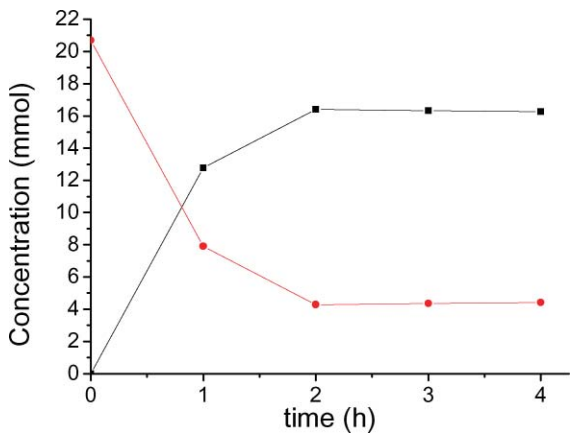

Fig. 6 $CoCl_2 \cdot 6H_2O$-catalyzed vanillyl alcohol oxidation: mmol of substrate and products *versus* time: (–●–) vanillyl alcohol; (–■–) vanillin. Reaction conditions: 5.00 g EMIM DEP, 10 μmol $CoCl_2 \cdot 6H_2O$ (0.0024 g), 1 mmol NaOH (0.04 g), 21.7 mmol vanillyl alcohol (3.189 g), 0.5 MPa O_2 (continuous), $T = 353$ K.

Veratryl alcohol (3,4-dimethoxybenzyl alcohol) (**8**), is a secondary metabolite synthesized from the degradation of lignin by the white rot fungus.[57,58] It has been widely used as a non-phenolic lignin model compound for the analysis of processes for catalytic lignin oxidation.[52,53,57,59] The functional groups present in this compound and ease of analysis make it a suitable compound for the investigation of catalytic oxidation capability. Thus, several catalytic systems have been reported for the oxidation of veratryl alcohol as a lignin model compound.[1] The extensive use of veratryl alcohol to test for oxidation capability by metalloporphrins and other catalysts allows facile comparison of catalyst activity and selectivity, which are important for further catalyst development. We therefore investigated the influence of reaction conditions using veratryl alcohol with the expectation that the results would extend to the other substrates as well.

The $CoCl_2 \cdot 6H_2O$-catalyzed veratryl alcohol oxidation was conducted in EMIM DEP under constant oxygen pressure in order to further analyze the ability of the catalyst to oxidize benzyl alcohol functionality in lignin. The results of the oxidation are given in Fig. 7. The $CoCl_2 \cdot 6H_2O$ catalyst precursor rapidly oxidized veratryl alcohol to veratraldehyde with a maximum turnover frequency of 1440 h^{-1}. The highest veratraldehyde yield was attained at 4 h, which corresponded to 3345 total catalytic turnovers. Similar results were obtained when $CoCl_2 \cdot 6H_2O$ was substituted with Co(salen), although slightly reduced maximum turnover frequencies were obtained (1300 h^{-1}). The formation of veratrylic acid was detected and coincided with the disappearance of veratraldehyde after 4 h. Little acid was detected at short reaction times when the veratraldehyde concentrations were low. These results, and the lack of acid at low substrate concentrations, as further discussed below, suggest that the acid forms by a series of reactions, whereby veratryl alcohol is first oxidized to veratraldehyde followed by over-oxidation to veratrylic acid.

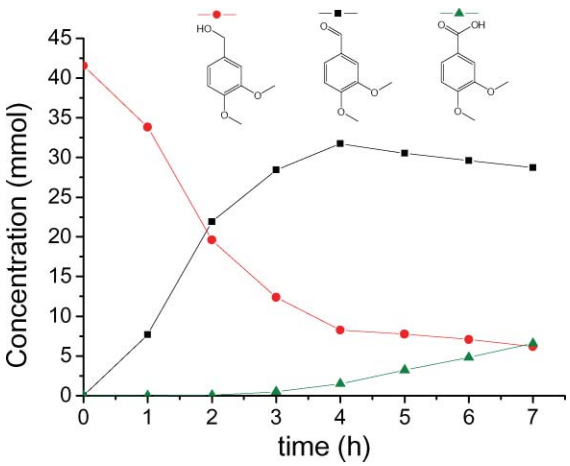

Fig. 7 Semi-batch $CoCl_2 \cdot 6H_2O$-catalyzed veratryl alcohol oxidation with high concentrations of veratryl alcohol: mmol of substrate and products *versus* time. Reaction conditions: 41.5 mmol veratryl alcohol (6.98 g), 0.5 MPa O_2 (continuous), $T = 353$ K.

Based on the high activity still observed at low oxygen pressure (see below), a semi-batch reaction at a lower oxygen pressure was conducted to determine the effect on the acid formation. The results are depicted in Fig. 8. The oxidation of veratryl alcohol still proceeded readily at low oxygen pressures, although the catalyst turnover frequency was slightly lower (790 h^{-1}). Importantly, significantly less acid was formed even as the concentration of veratraldehyde increased. These results indicate that the susceptibility of the catalytic system to over-oxidize veratryl alcohol can be tuned based on the oxygen pressure, effectively increasing selectivity to veratraldehyde with little loss of activity.

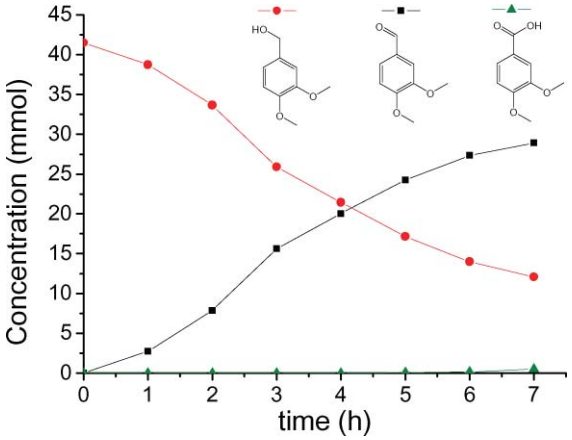

Fig. 8 Semi-batch $CoCl_2 \cdot 6H_2O$-catalyzed veratryl alcohol oxidation with high concentrations of veratryl alcohol at lower oxygen pressures: mmol substrate and products *versus* time. Reaction conditions: 41.5 mmol veratryl alcohol (6.98 g), 0.1 MPa O_2 (continuous), T = 353 K.

The performance of this catalytic system for veratryl alcohol oxidation contrasts with biomimetic metalloporphyrin and metallosalen complexes, which have also been extensively used to study veratryl alcohol oxidation. The oxidation rate was significantly higher (two orders of magnitude) in the present system relative to both of the previously reported catalysts, Co(salen) and Co(porphyrin), which are both known to reversibly bind molecular oxygen and subsequently oxidize veratryl alcohol. Turnover frequencies for the former are typically between 10–15 h^{-1} with total turnover numbers of 300,[36–38,60] and although 100% veratryl alcohol conversion was achieved, the total turnover numbers for Co(porphyrin) catalysts were only ~33 in total in 12 h.[33] Different product distributions were also obtained. With iron or manganese porphyrin catalysts (which use H_2O_2 as the oxidant[61]), and Co(porphyrins) (which use molecular oxygen[33,62]), quinones were detected as reaction products[33,63] in addition to veratraldehyde and veratrylic acid.[52,53,63,64] Only veratraldehyde and veratrylic acid were obtained as products with $CoCl_2 \cdot 6H_2O$ or Co(salen) in EMIM DEP.

3.4 Catalysts, ligands, and other reaction conditions

The accumulated evidence indicated above suggests that $CoCl_2 \cdot 6H_2O$ in EMIM DEP acts as a mild but efficient oxidation catalyst capable of increasing the oxygen functionality in lignin. As indicated above, Co(salen) complexes are also active in EMIM DEP for catalytic oxidation. The effectiveness of this and similar complexes as oxidation catalysts have been studied in organic[35] and aqueous solutions, and the effects of reaction conditions, including temperature,[60] the presence of NaOH,[37] and oxygen pressure,[60] have been studied in detail. The reversible reaction of Co(salen) with oxygen gives an equilibrium mixture of Co-superoxo complex and the dimeric peroxo complex with the relative proportion strongly depending on the nature of the starting complex and the reaction conditions.[34,65] Moreover, the ability of the Co complex to bind oxygen is strongly affected by the coordination environment around the cobalt. Poor oxygen binding occurs with 4-coordinate complexes but strong binding occurs with 5-coordinate complexes.[34] This extensive literature precedence provides a convenient point of comparison in order to elucidate the behavior of the Co catalysts in the unique environment provided by the EMIM DEP.

3.4.1 Reactions in other ionic liquids. The imidazolium ionic liquids have several distinctive properties that could potentially result in the higher activity observed in the EMIM DEP, as determined by the oxidation rate of the model compounds indicated above, relative to other solvents. Ionic liquids are known to exhibit high gas solubilities[50,51] especially relative to water. The increased oxidation rates may result because of the increased oxidation potential caused by the higher oxygen content in the ionic liquid. This possibility was explored and is discussed below. Next, the ionic liquids themselves are typically only 98% pure, and the remaining impurities, which are in large excess relative to the catalyst, could influence the catalytic activity. A third possibility for the higher activity originates from the interaction of the anionic component of the ionic liquid with the catalyst.

In order to probe the role of the ionic liquid, and the impurities contained therein, on catalytic performance, the oxidation of veratryl alcohol was performed in the ionic liquids EMIM CH_3SO_3 and BMIM PF_6, in addition to EMIM DEP. The results of the veratryl alcohol oxidation using Co(salen) in these ionic liquids are depicted in Fig. 9. The oxidation using water as a solvent was included for comparison purposes, in which about 24% of the veratryl alcohol was oxidized in 18 h. In each case, the only product detected was veratraldehyde. Analysis of catalytic performance in these exemplary ionic liquids yields valuable insight regarding the role of the impurities contained in the ionic liquids and anionic content as possible reasons for the increased activity. Firstly, the identities of the impurities in each ionic liquid were determined by ethyl acetate extraction and analysis by GC-MS. In all cases, the presence of methylimidazole was detected as the primary impurity in addition to residual unreacted anionic components (*i.e.* $PO_4(C_2H_5)_3$ in the case of DEP). Axial ligands, such as imidazole or pyridine, are known to enhance the activity of Co(salen)[60] and Co(porphyrin) complexes;[66] however, if the imidazole impurity was solely responsible for the enhanced activity, similarly high activity would occur for the EMIM DEP, EMIM CH_3SO_3 and BMIM PF_6 ionic liquids because they contain similar impurities. As seen in Fig. 8, vastly different activity was observed in these ionic liquids; thus, the presence

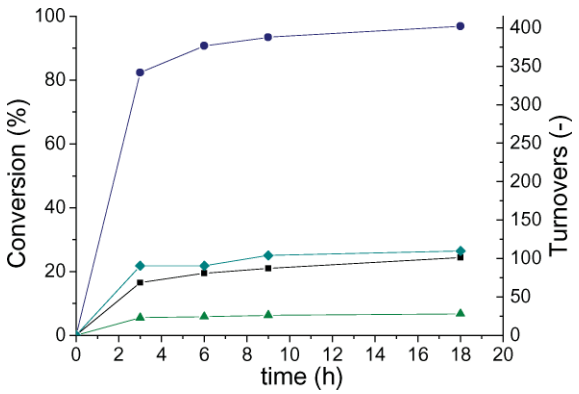

Fig. 9 Conversion of veratryl alcohol to veratraldehyde and Co(salen) turnovers *versus* time using various ionic liquids as solvents: (–■–) H_2O; (–●–) EMIM DEP; (–◆–) EMIM CH_3SO_3; (–▲–) BMIM PF_6.

of these impurities can be eliminated as a potential cause of the higher activity observed in EMIM DEP. Comparison of the results in which the cationic portion of the ionic liquid remained constant whereas the anionic component was altered, *i.e.* with EMIM DEP and EMIM CH_3SO_3, indicates instead that the choice of ionic liquid anion plays a significant role in the performance of the Co(salen) catalyst. With EMIM DEP, a high oxidation rate was observed. whereas with EMIM CH_3SO_3 the rate of veratryl alcohol oxidation was only slightly higher than that observed in water. In addition, the hexafluorophosphate component of BMIM PF_6 is generally accepted as a weakly-coordinating anion[8] and is therefore not expected to interact strongly with the catalyst. The catalytic activity in this ionic liquid, however, was lower even than in water, as indicated in Fig. 8. The accumulated evidence suggests that interaction of the diethyl phosphate component of the ionic liquid with the transition metal cation is an important factor for the high activity observed in EMIM DEP.

3.4.2 Influence of oxygen pressure. As indicated above, another plausible explanation for the high oxidation rates in ionic liquids originated with the high gas solubility relative to other solvents, such as water. In order to explore this possibility, the influence of oxygen pressure on catalytic performance was investigated. Fig. 10 indicates the influence of oxygen pressure on veratryl alcohol conversion and catalyst turnovers. Without molecular oxygen present, no veratryl alcohol oxidation was observed. As indicated in Fig. 9, the oxidation reaction proceeded at relatively low oxygen pressures, where nearly 80% of the veratryl alcohol was oxidized to veratraldehyde with 0.125 MPa O_2. Further increases in the oxygen pressure resulted in slight but monotonic increases in catalytic activity. These results suggest a high oxidation potential in the ionic liquid even at low oxygen pressures, which allows the lignin oxidation to occur under very mild conditions. The high oxygen solubility in the EMIM DEP relative to other solvents is thus an important contributing factor for the high activity observed. Moreover, the ability to use low gas pressure is attractive for use in a biorefinery because of decreased capital costs and increased process safety associated with lower pressures.

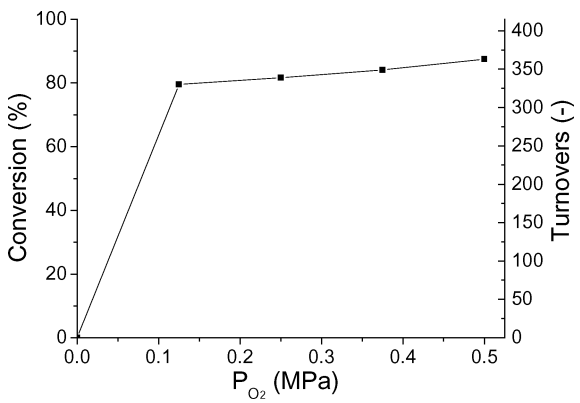

Fig. 10 Conversion of veratryl alcohol to veratraldehyde and catalyst turnover numbers *versus* oxygen pressure. Reaction conditions: 5.00 g EMIM DEP, 5 μmol Co(salen) (0.0016 g), 1 mmol NaOH (0.04 g), 2.08 mmol veratryl alcohol (0.349 g), $T = 353$ K, $t = 3$ h. At 0.0 MPa P_{O_2}, N_2 was used to purge the autoclave rather than O_2.

3.4.3 Effect of reaction temperature. The preceding examples indicate that Co(salen) dissolved in EMIM DEP catalyzes oxidation reactions at faster rates using lower oxygen pressures than the same catalyst dissolved in other solvents. In order to determine if the Co(salen)–EMIM DEP system was also capable of performing oxidations at reduced and elevated temperatures, the influence of temperature on veratryl alcohol oxidation was investigated. The results are depicted in Fig. 11. At and below 323 K, no veratryl alcohol oxidation was observed. In accordance with previous reports of Co(salen) performance in water, temperatures exceeding 343 K are required for high catalytic activity.[60] Increases in catalytic activity were observed as the temperature was increased up to 383 K, when nearly 100% of the veratryl alcohol was consumed after 3 h. Increasing the temperature to 413 K had a deleterious effect on the catalytic system. An orange-brown solid formed, the color of the ionic liquid changed to dark red, and the viscosity of the solution was increased. Not all of the products formed as a result of the veratryl alcohol oxidation were recovered, thus indicating that a portion of the solid observed formed as a result of the reaction of the veratryl alcohol, possibly as a polymerization reaction. The optimal range for the selective veratryl alcohol oxidation therefore fell between 353 and 383 K. These results suggest that elevated temperatures are still required for the formation of the catalytically active species in accordance with previous reports of Co(salen) in other solvents.

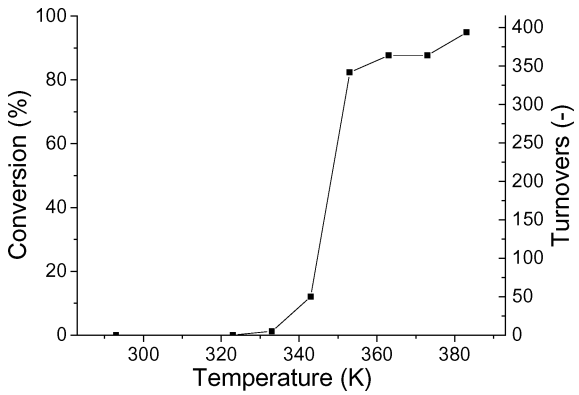

Fig. 11 Conversion and catalytic turnovers *versus* temperature. Reaction conditions: 5.00 g EMIM DEP, 5 μmol Co(salen) (0.0016 g), 1 mmol NaOH (0.04 g), 2.08 mmol veratryl alcohol (0.349 g), 0.5 MPa O_2, $t =$ 3 h.

3.4.4 Influence of NaOH. NaOH is an important component of the reaction system for Co(salen) catalyzed oxidations.[37] In aqueous solutions, a hydroxide anion acts as an axial ligand that facilitates coordination with molecular oxygen.[37] Preliminary experiments of Co(salen) in EMIM DEP indicate that NaOH is also important; however, the role of NaOH in the EMIM DEP was not immediately clear. The importance of NaOH for the Co(salen)-catalyzed veratryl alcohol oxidation in EMIM DEP was therefore investigated to determine the role of $^-$OH and to determine whether it was catalytic or if it was consumed during the course of the reaction. Firstly, reactions in which high substrate quantities were dissolved in the ionic liquids were conducted. Table 1 depicts the conversion of veratryl alcohol to veratryl aldehyde using high initial

Table 1 Batch conversion of veratryl alcohol to veratryl aldehyde with high substrate concentrations (41.5 mmol, 6.98 g). Amount of O_2 estimated using ideal gas law: $P = 0.6$ MPa, $V = 0.04$ L, $T = 298$ K. Oxygen recharged to autoclave between samples

Entry	Time/h	Starting O_2/mmol	NaOH/mmol	Conversion (%)	Veratryl alcohol consumed/mmol	Total aldehyde/NaOH ratio	Aldehyde/O_2 ratio	Aldehyde/O ratio
1	3	9.8	2.0	41.7	17.3	8.7	1.8	0.9
2	6	9.8	2.0	72.2	12.7	15.0	1.3	0.6
3	9	9.8	2.0	82.5	4.3	17.2	0.4	0.2
4	18	9.8	2.0	86.9	1.8	18.1	0.2	0.1

substrate concentrations. After three hours reaction (Entry 1), the reactor pressure dropped to nearly zero, and analysis of the reaction solution indicated that 41.7% of the veratryl alcohol was oxidized to veratraldehyde, corresponding to 17.3 mmol of substrate consumed. The ratio of the total quantity of aldehyde produced to the quantity of NaOH charged to the autoclave indicated an 8.7-fold excess of veratraldehyde to NaOH. The stoichiometry suggests that NaOH is not consumed during the course of the reaction, but instead merely facilitates the oxidation. In addition, veratryl alcohol oxidation did not occur in the absence of molecular oxygen even with NaOH present (see above), further indicating that molecular oxygen is the ultimate oxidant rather than the oxygen contained in the $^-$OH anion. Furthermore, an estimate of the quantity of oxygen initially charged to the autoclave using the ideal gas law indicated an approximately 2 : 1 molecular ratio of aldehyde was produced to oxygen consumed. For other Co(salen) oxidations, both H_2O_2[36,37,39] and H_2O[38] have been reported as reaction by-products. These results suggest, by stoichiometry, that the ultimate by-product of the oxidation conducted by Co(salen) in EMIM DEP is water rather than hydrogen peroxide, and also that both atoms of the oxygen molecule are ultimately consumed in the reaction. The conversion of veratryl alcohol increased with increasing reaction time, as indicated by Entries 2–4, ultimately culminating in 86.9% conversion after 18 h.

During Co(salen)-catalyzed reactions in water, $^-$OH was found to bond axially to the Co complex, which served to activate it.[37,60] In the presence of $^-$OH anions, other components such as pyridine, which normally increases the activity of the complex, were unnecessary.[60] Likewise, NaOH was an important component of the reaction system for Co(salen) in EMIM DEP. As indicated in Fig. 12, after 3 h no veratryl alcohol oxidation was observed in the absence of NaOH, and the catalytic activity increased as the NaOH concentration increased, approaching nearly complete veratryl alcohol conversion at the highest NaOH concentrations. As indicated above, the $^-$OH anions were not consumed as a stoichiometric reactant relative to veratryl alcohol, suggesting that NaOH plays a role in activating the catalyst instead. Several of the metal complexes investigated in this study (discussed in detail below) have a vastly different coordination environment than Co(salen) and therefore could potentially behave significantly differently relative to Co(salen). For example, with the exception of the Co(porphyrin) complex and Jacobsen's catalyst, none of the other complexes analyzed for oxidative capability have a square-planar geometry. They therefore lack the axial position through which to bond $^-$OH such that molecular oxygen would bond *trans* to the $^-$OH while leaving the other ligands in the complex in their original positions. One of the most active catalyst precursors, $CoCl_2{\cdot}6H_2O$,

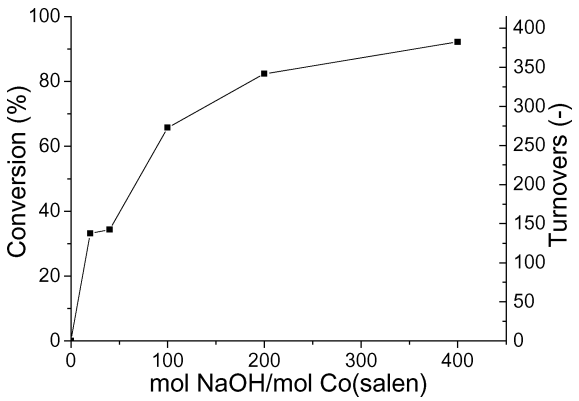

Fig. 12 Conversion of veratryl alcohol and catalyst turnovers *versus* time with added NaOH. Reaction conditions: 5.00 g EMIM DEP, 5 μmol Co(salen) (0.0016 g), 2.08 mmol veratryl alcohol (0.349 g), 0.5 MPa O_2, $T = 353$ K, $t = 3$ h.

has a distinctly different coordination environment relative to the Co(salen) complex. In the ionic liquid, $CoCl_2{\cdot}6H_2O$ adopts a tetrahedral geometry with distinct d-to-d transitions in the visible region, giving the complex a green-blue color, whereas the higher-energy d-to-d transitions for the square-planar Co(salen) complex give it a yellow color in solution. In other solvents, the different ligand environment causes vastly different reactivity between the complexes. As noted earlier, when dissolved in water, Co(salen) oxidizes veratryl alcohol, whereas no oxidation was observed when $CoCl_2{\cdot}6H_2O$ was used as the catalyst. Nevertheless, in EMIM DEP, $CoCl_2{\cdot}6H_2O$ oxidized veratryl alcohol more rapidly than the Co(salen) complex. In order to determine if this difference in coordination environment would similarly influence the role of $^-$OH, reactions catalyzed by $CoCl_2{\cdot}6H_2O$ in the absence of NaOH were conducted, and the results are depicted in Fig. 13. As in the case of the Co(salen), the oxidation of veratryl alcohol was not observed initially. Remarkably, after an approximately 5 h induction period, $CoCl_2{\cdot}6H_2O$ began to oxidize the veratryl alcohol, and the rate soon approached the rate observed with the catalyst in the presence of NaOH. The solution color at the conclusion of the reaction, as determined by UV-visible spectroscopy, strongly resembled the solution after the reaction in which NaOH was present. When the experiment was repeated using Co(salen) as the catalyst, a similar result was obtained. After the same induction period, the oxidation of veratryl alcohol proceeded. As indicated in Fig. 14, the change in activity coincided with a change in the color of the reaction solution from green, in the case of $CoCl_2{\cdot}6H_2O$, to yellow and finally orange. The onset of activity was marked by the appearance of a strong absorbance near 345 nm, which indicated a change in the coordination sphere of the catalyst.

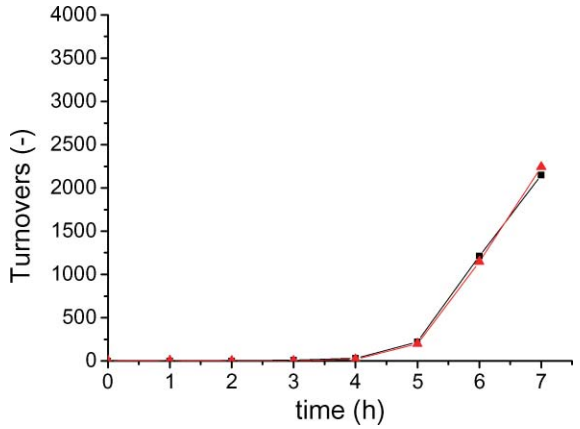

Fig. 13 Catalyst turnovers *versus* time for the oxidation of veratryl alcohol in the absence of NaOH. (–■–) $CoCl_2 \cdot 6H_2O$; (–▲–) Co(salen).

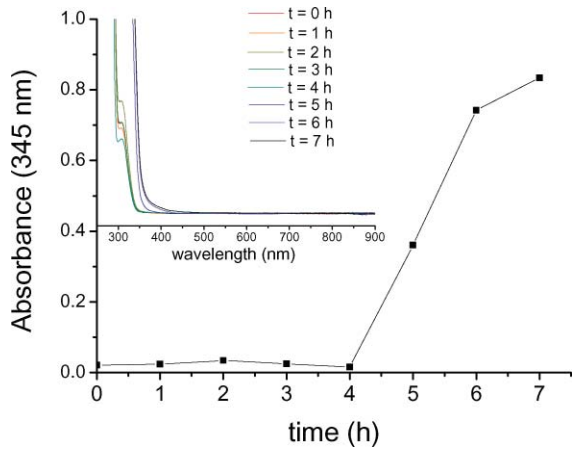

Fig. 14 Absorbance at 345 nm *versus* time for $CoCl_2 \cdot 6H_2O$-catalyzed veratryl alcohol oxidation in the absence of NaOH. The inset graph depicts the full spectrum at various reaction times.

Both the Co(salen) and $CoCl_2 \cdot 6H_2O$ reverted to the same color, and the UV-visible spectrum of the final solution was indistinguishable with $CoCl_2 \cdot 6H_2O$- and Co(salen)-catalyzed reactions in the presence of NaOH at shorter reaction times. The similar rate observed in the presence of NaOH, and in its absence after the induction period, indicates that NaOH does not assist the reaction by deprotonating the substrate, making the substrate more reactive. If, in fact, NaOH was necessary to deprotonate the substrate, a significantly lower rate would be expected even after the induction period in the absence of NaOH. Taken together with the other observations of NaOH indicated above, these results suggest instead that the presence of ^-OH accelerates the formation of the active catalytic complex in the EMIM DEP solution rather than serving as an actual ligand on the Co complex itself. After a suitable induction period, the Co catalyst still reverts to the same active form even in the absence of NaOH, as indicated by the UV-visible spectrum of the complex after reaction.

3.4.5 Other transition metal catalysts. Although the most active, Co catalysts were not the only transition metals capable of acting as an oxidation catalyst in the EMIM DEP. Fig. 15 depicts the conversion of veratryl alcohol to veratryl aldehyde and catalyst turnovers at various reaction times in EMIM DEP using a wide range of other transition metals. The transition metal salts tested included: a) cobalt porphyrin, Co(salen), and simpler Co salts; b) Mn-based Jacobsen's catalyst, which is usually used in conjunction with H_2O_2 or other peroxides that are thought to generate high-valent oxomanganese species,[67,68] and simpler Mn salts; c) Fe salts; d) Cr salts; e) Ni salts; and finally f) Cu salts. The activity of Co(salen) is included in all graphs to aid in comparison of relative activities. In all cases, the only product observed was veratraldehyde. Several of the simpler Co salts, including $CoCl_2 \cdot 6H_2O$, $Co(acac)_3$, $Co(acac)_2$, $Co(OAc)_2 \cdot 4H_2O$, and $Co(NO_3)_2 \cdot 6H_2O$, provided slightly higher activity than the Co(salen) complex and significantly outperformed the Co porphyrin catalyst. These results were surprising since the latter compounds are known to engage in the selective oxidation of veratryl alcohol to veratraldehyde.[33] Nearly 90% conversion of the veratryl alcohol was achieved after 3 h, and in many cases the reaction was driven nearly to completion at longer reaction times with these catalysts. In contrast, only approximately 80% and 10% of the starting veratryl alcohol was oxidized to veratraldehyde with the Co(salen) and Co porphyrin complex, respectively; the remainder was recovered as starting material. A similar occurrence was observed with the Mn-catalyzed reactions, as indicated by Fig. 15b. Veratryl alcohol oxidation was observed when catalyzed by simpler Mn salts (namely $Mn(NO_3)_2$ and $Mn(OAc)_2$), but Jacobsen's catalyst (a Mn–Schiff base epoxidation catalyst that resembles the Co(salen) structure) was ineffective for veratryl alcohol oxidation. In general, the compounds with tetradentate ligands exhibited reduced activity, suggesting that these strongly-binding ligands block a coordination site on the catalyst center or, alternatively, are resistant to transformation of the metal center to its active form.

Veratryl alcohol oxidation was also observed with complexes of Fe, Cr, and Ni, as indicated in Fig. 15c–e.

Relatively high activity was observed with $Cr(acac)_3$, which was less effective than Co, yet conversion of veratryl alcohol approached 100% at longer times. Activity was also observed with complexes of Fe and Ni, with approximately 50% of the starting material oxidized to veratraldehyde with the Fe catalysts and approximately 30% oxidized with Ni. In contrast, Cu was an ineffective oxidation catalyst; there was no indication of any reaction, and only the starting material was recovered.

These results indicate that several transition metal catalysts are capable of oxidizing veratryl alcohol to veratraldehyde when EMIM DEP is used as the solvent. The general order of activity for the transition metal cations investigated was Co > Cr > Fe > Ni > Mn ≫ Cu, although some variations existed depending on the starting complex. The EMIM DEP proved an important solvent for the use of these transition metals as oxidation catalysts. All of the salts investigated readily dissolved in the ionic liquid after stirring overnight, whereas several of the salts failed to dissolve in other solvents, such as water. The reactivity of these salts was also significantly different in EMIM DEP relative to other solvents such as water. For example, although the Co(salen) complex is capable of performing veratryl alcohol oxidation in water, as indicated in Fig. 9 and previous reports,[38,60] no oxidation was observed when $Co(OAc)_2 \cdot 4H_2O$ and $CoCl_2 \cdot 6H_2O$ were used in water, yet

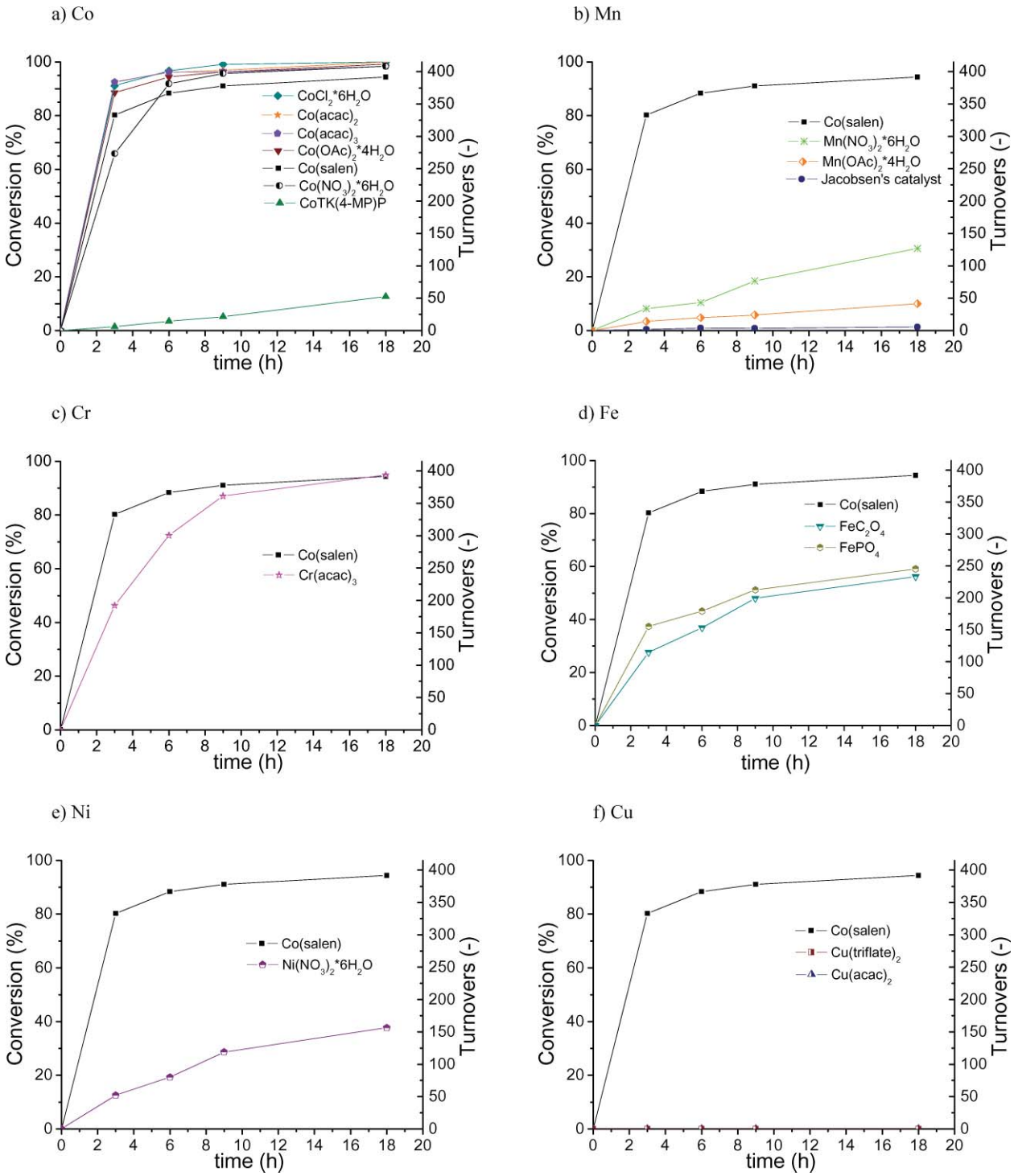

Fig. 15 Conversion of veratryl alcohol to veratraldehyde and catalyst turnovers *versus* time using 10 μmol of various transition metal catalysts. CoTK(4-MP) P = 5,10,15,20-tetrakis(4-methoxyphenyl)-21*H*,23*H*-porphyrin cobalt(II). Jacobsen's catalyst = (*R*,*R*)-(−)-*N*,*N*′-bis(3,5-di-*tert*-butylsalicylidene)-1,2-cyclohexane-diaminomanganese(III) chloride.

these salts proved excellent precursors for highly active oxidation catalysts when dissolved in EMIM DEP.

4. Conclusions

Taken together, the results of the lignin model compound analysis coupled with the spectroscopic evidence obtained during the lignin oxidation provide insight regarding the lignin oxidation. The inability of the catalyst to disrupt the β-*O*-4, 5–5′, and other linkages present in the model compounds suggests that these linkages remained intact during the lignin oxidation. These results indicate the reason that the low molecular weight monomeric compounds were not detected as a result of the oxidation. Similarly, phenolic functional groups remained intact,

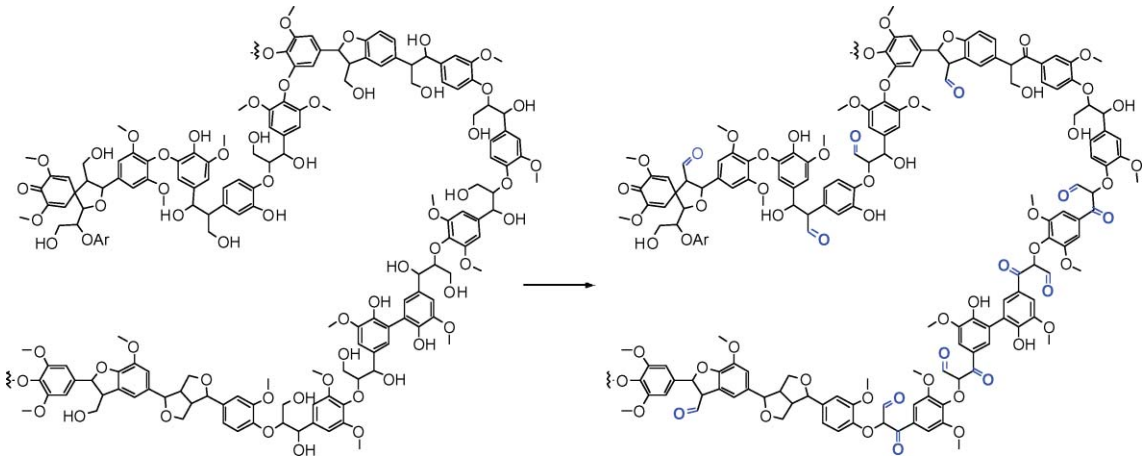

Scheme 2 Possible structural changes in lignin samples as a result of oxidation.

but benzyl and other alcohol functionalities were susceptible to oxidation to form aldehydes or, with high oxygen pressures or substrate loadings, to over-oxidation, forming acids. These oxidations proceed at high rates under mild conditions. A schematic representation of the possible transformations in the lignin that resulted are given in Scheme 2. The transformations indicated in the scheme represent several of the anticipated changes based on the results of the lignin model compounds and spectroscopic analysis. The ether and carbon–carbon linkages remain intact, but several of the alcohol functional groups in the lignin are oxidized to the corresponding aldehyde.

The EMIM DEP and Co catalyst combination proved suitable for lignin and lignin model compound oxidation using molecular oxygen. Properties of the ionic liquid, including high oxygen solubility, allowed the oxidation to proceed under mild conditions, and the large abundance of diethyl phosphate anion caused simple metal salts to exhibit remarkably high activity. Catalyst precursors with strongly binding ligands, such as tetradentate porphryin or salen ligands, tended to exhibit reduced activity relative to simple metal salts, which suggests that these strongly-binding ligands inhibit the transformation of the transition metal to the active form, which is a process aided by the presence of $^{-}$OH anions. Nevertheless, the ionic liquid EMIM DEP provided a suitable media for the dissolution and subsequent oxidation of lignin, or molecules derived therefrom, using a variety of transition metal catalysts. This catalyst system could potentially be used as a lignin pretreatment method in a biorefinery to increase the functionality and hydrophilic character of the lignin, prior to a subsequent step designed to rupture the lignin linkages to yield highly-functionalized monomers. Alternatively, given the high oxidation rate relative to similar catalysts in common aqueous or organic solvents, it could be used as a secondary step to functionalize the compounds formed after the pretreatment step that forms the lignin monomers.

Acknowledgements

JZ gratefully thanks the National Science Foundation International Research Fellowship Program for support of this research under Award No. 0856754. Thanks are also extended to Richard Gosselink of Wageningen UR Food & Biobased Research and to Wouter Huijgen of ECN for supplying the Alcell and soda lignin, respectively.

References

1 J. Zakzeski, P. C. A. Bruijnincx, A. L. Jongerius and B. M. Weckhuysen, *Chem. Rev.*, 2010, 10.1021/cr900354u.
2 C. Hill, *Wood modification. Chemical, Thermal, and Other Processes*, John Wiley & Sons, Chichester, 2006.
3 F. S. Chakar and A. J. Ragauskas, *Ind. Crops Prod.*, 2004, **20**, 131–141.
4 R. D. Perlack, L. L. Wright, A. F. Turhollow, R. L. Graham, B. J. Stokes and D. C. Erbach, *Biomass as Feedstock for a Bioenergy and Bioproducts Industry: The Technical Feasibility of a Billion-Ton Annual Supply*, U.S. Dept. of Energy and U.S. Dept. of Agriculture, Oak Ridge National Laboratory, Oak Ride, Tennessee, 2005, pp. 1–59.
5 S. K. Ritter, *Chem. Eng. News*, 2008, **86**, 10–17.
6 M. Fasching, P. Schröder, R. P. Wollboldt, H. K. Weber and H. Sixta, *Holzforschung*, 2008, **62**, 15–23.
7 C. Eckert, C. Liotta, A. Ragauskas, J. Hallett, C. Kitchens, E. Hill and L. Draucker, *Green Chem.*, 2007, **9**, 545–548.
8 I. Krossing and I. Raabe, *Angew. Chem., Int. Ed.*, 2004, **43**, 2066–2090.
9 R. A. Sheldon, R. M. Lau, M. J. Sorgeddrager and F. van Rantwijk, *Green Chem.*, 2002, **4**, 147–151.
10 S. H. Lee, T. V. Doherty, R. J. Linhardt and J. S. Dordick, *Biotechnol. Bioeng.*, 2009, **102**, 1368–1376.
11 D. A. Fort, R. C. Remsing, R. P. Swatloski, P. Moyna, M. Guillermo and R. D. Rogers, *Green Chem.*, 2007, **9**, 63–69.
12 M. Zavrel, D. Bross, M. Funke, J. Büchs and A. C. Spiess, *Bioresour. Technol.*, 2009, **100**, 2580–2587.
13 N. Sun, M. Rahman, Y. Qin, M. L. Maxim, H. Rodríquez and R. D. Rogers, *Green Chem.*, 2009, **11**, 646–655.
14 Y. Pu, N. Jiang and A. J. Ragauskas, *J. Wood Chem. Technol.*, 2007, **27**, 23–33.
15 S. S. Y. Tan, D. R. MacFarlane, J. Upfal, L. A. Edye, W. O. S. Doherty, A. F. Patti, J. M. Pringle and J. L. Scott, *Green Chem.*, 2009, **11**, 339–345.
16 J. Vitz, T. Erdmenger, C. Haensch and U. S. Schubert, *Green Chem.*, 2009, **11**, 417–424.
17 M. E. Zakrzewska, E. Bogel-Lukasik and R. Bogel-Lukasik, *Energy Fuels*, 2010, **24**, 737–745.
18 I. Kilpelaeinen, H. Xie, A. King, M. Granstrom, S. Heikkinen and D. S. Argyropoulos, *J. Agric. Food Chem.*, 2007, **55**, 9142–9148.
19 C. Sievers, M. B. Valenzuela-Olarte, T. Marzialetti, I. Musin, P. K. Agrawal and C. W. Jones, *Ind. Eng. Chem. Res.*, 2009, **48**, 1277–1286.
20 C. Li, Q. Wang and Z. K. Zhao, *Green Chem.*, 2008, **10**, 177–182.
21 H. Xie, A. King, I. Kilpelainen, M. Granstrom and D. S. Argyropoulos, *Biomacromolecules*, 2007, **8**, 3740–3748.

22 J. B. Binder, M. J. Gray, J. F. White, Z. C. Zhang and J. E. Holladay, *Biomass Bioenergy*, 2009, **33**, 1122–1130.
23 S. Sgalla, G. Fabrizi, S. Cacchi, A. Macone, A. Bonamore and A. Boffi, *J. Mol. Catal. B: Enzym.*, 2007, **44**, 144–148.
24 F. G. Sales, L. C. A. Maranhão, N. M. Lima Filho and C. A. M. Abreu, *Chem. Eng. Sci.*, 2007, **62**, 5386–5391.
25 S. Bhargava, H. Jani, J. Tardio, D. Akolekar and M. Hoang, *Ind. Eng. Chem. Res.*, 2007, **46**, 8652–8656.
26 J. Zhang, H. Deng and L. Lin, *Molecules*, 2009, **14**, 2747–2757.
27 R. DiCosimo and H. C. Szabo, *J. Org. Chem.*, 1988, **53**, 1673–1679.
28 G. A. A. Labat and A. R. Goncalves, *Appl. Biochem. Biotechnol.*, 2008, **148**, 151–161.
29 A. R. Gonçalves and U. Schuchardt, *Appl. Biochem. Biotechnol.*, 1999, **77**, 127–132.
30 W. Partenheimer, *Adv. Synth. Catal.*, 2009, **351**, 456–466.
31 S. Hwang, Y.-W. Lee, C.-H. Lee and I.-S. Ahn, *J. Polym. Sci., Part A: Polym. Chem.*, 2008, **46**, 6009–6015.
32 V. E. Tarabanko, N. A. Fomova, B. N. Kuznetsov, N. M. Ivanchenko and A. V. Kudryashev, *React. Kinet. Catal. Lett.*, 1995, **55**, 161–170.
33 W. Zhu and W. T. Ford, *J. Mol. Catal.*, 1993, **78**, 367–378.
34 J. J. Bozell, B. R. Hames and D. R. Dimmel, *J. Org. Chem.*, 1995, **60**, 2398–2404.
35 R. S. Drago, B. B. Corden and C. W. Barnes, *J. Am. Chem. Soc.*, 1986, **108**, 2453–2454.
36 V. Sippola, O. Krause and T. Vuorinen, *J. Wood Chem. Technol.*, 2004, **24**, 323–340.
37 K. Kervinen, M. Allmendinger, M. Leskelä, T. Repo and B. Rieger, *Phys. Chem. Chem. Phys.*, 2003, **5**, 4450–4454.
38 K. Kervinen, H. Korpi, J. G. Mesu, F. Soulimani, T. Repo, B. Rieger, M. Leskelä and B. M. Weckhuysen, *Eur. J. Inorg. Chem.*, 2005, 2591–2599.
39 C. Canevali, M. Orlandi, L. Pardi, B. Rindone, R. Scotti, J. Sipila and F. Morazzoni, *J. Chem. Soc., Dalton Trans.*, 2002, 3007–3014.
40 J. A. F. Gamelas, A. R. Gaspar, D. V. Evtuguin and C. Pascoal Neto, *Appl. Catal., A*, 2005, **295**, 134–141.
41 A. Gaspar, D. V. Evtuguin and C. Pascoal Neto, *Appl. Catal., A*, 2003, **239**, 157–168.
42 A. R. Gaspar, J. A. F. Gamelas, D. V. Evtuguin and C. P. Neto, *Chem. Eng. Commun.*, 2009, **196**, 801–811.
43 Y. S. Kim, H.-m. Chang and J. F. Kadla, *J. Wood Chem. Technol.*, 2007, **27**, 225–241.
44 T. Yokoyama, H.-m. Chang, R. S. Reiner, R. H. Atalla, I. A. Weinstock and J. F. Kadla, *Holzforschung*, 2004, **58**, 116–121.
45 T. Voitl and P. R. von Rohr, *ChemSusChem*, 2008, **1**, 763–769.
46 A. Gaspar, D. V. Evtuguin and C. P. Neto, *Holzforschung*, 2004, **58**, 640–649.
47 H. Deng, L. Lin, Y. Sun, C. Pang, J. Zhuang, P. Ouyang, Z. Li and S. Liu, *Catal. Lett.*, 2008, **126**, 106–111.
48 H. Deng, L. Lin, Y. Sun, C. Pang, J. Zhuang, P. Ouyang, J. Li and S. Liu, *Energy Fuels*, 2009, **23**, 19–24.
49 B. N. Kuznetsov, V. E. Taraban'ko and S. A. Kuznetsova, *Kinet. Catal.*, 2008, **49**, 517–526.
50 J. Palgunadi, J. E. Kang, D. Q. Nguyen, J. H. Kim, B. K. Min, S. D. Lee, H. Kim and H. S. Kim, *Thermochim. Acta*, 2009, **494**, 94–98.
51 A. Finotello, J. E. Bara, D. Camper and R. D. Noble, *Ind. Eng. Chem. Res.*, 2008, **47**, 3453–3459.
52 G. Labat and B. Meunier, *J. Org. Chem.*, 1989, **54**, 5008–5011.
53 F. Cui and D. Dolphin, *Bioorg. Med. Chem.*, 1995, **3**, 471–477.
54 F. A. Marques, F. Simonelli, A. R. M. Oliveira, G. L. Gohr and P. C. Leal, *Tetrahedron Lett.*, 1998, **39**, 943–946.
55 M. Albrecht and M. Schneider, *Synthesis*, 2000, 1557–1560.
56 S. Kawai, K. Okita, K. Sugishita, A. Tanaka and H. Ohashi, *J. Wood Sci.*, 1999, **45**, 440–443.
57 K. Lee, K. Pi and K.-M. Lee, *World J. Microbiol. Biotechnol.*, 2009, **25**, 1691–1694.
58 J.-T. Liu, X.-R. Huang and P.-J. Gao, *Chin. J. Chem.*, 2007, **25**, 1627.
59 K. González Arzola, M. C. Arévalo and M. A. Falcón, *Electrochim. Acta*, 2009, **54**, 2621–2629.
60 K. Kervinen, H. Korpi, M. Leskelä and T. Repo, *J. Mol. Catal. A: Chem.*, 2003, **203**, 9–19.
61 M. Tien and T. K. Kirk, *Science*, 1983, **221**, 661–663.
62 P. Zucca, F. Sollai, A. Garau, A. Rescigno and E. Sanjust, *J. Mol. Catal. A: Chem.*, 2009, **306**, 89–96.
63 A. Kumar, N. Jain and S. M. S. Chauhan, *Synlett*, 2007, 411–414.
64 P. Zucca, G. Mocci, A. Rescigno and E. Sanjust, *J. Mol. Catal. A: Chem.*, 2007, **278**, 220–227.
65 K. C. Gupta, A. K. Sutar and C.-C. Lin, *Coord. Chem. Rev.*, 2009, **253**, 1926–1946.
66 M. Tsuda and H. Kasai, *Surf. Sci.*, 2007, **601**, 5200–5206.
67 T. Kurahashi and H. Fujii, *Inorg. Chem.*, 2008, **47**, 7556–7567.
68 C. M. M. Santos, A. M. S. Silva, J. A. S. Cavaleiro, A. Lévai and T. Patonay, *Eur. J. Org. Chem.*, 2007, 2877–2887.

